Dalton Transactions

Accepted Manuscript

ROYAL SOCIETY OF CHEMISTRY

www.rsc.org/dalton

Cite this: DOI: 10.1039/c0xx00000x

www.rsc.org/xxxxxx

ARTICLE TYPE

Synthesis, Characterization, Photophysics, and Anion Binding Properties of Platinum(II) Acetylide Complexes with Urea Group

Zhi-Hui Zhang, Jiewei Liu, Li-Qi Wan, Fang-Ru Jiang, Chi-Keung Lam, Bao-Hui Ye, Zhengping Qiao, and Hsiu-Yi Chao*

Received (in XXX, XXX) Xth XXXXXXXXX 20XX, Accepted Xth XXXXXXXXX 20XX
DOI: 10.1039/b000000x

Abstract: A new class of platinum(II) acetylide complexes with urea group, [Pt(^{t}Bu$_3$tpy)(C≡CC$_6$H$_4$-4-NHC(O)NHC$_6$H$_4$-4-R)](OTf) (^{t}Bu$_3$tpy = 4,4′,4″-tri-*tert*-butyl-2,2′:6′,2″-terpyridine; R = H (**3a**), Cl (**3b**), CF_3 (**3c**), and NO_2 (**3d**)), has been synthesized and characterized. The crystal structures of **3a**, **3a·DMF·THF**, **3b·CH$_3$CN**, and **3c·CH$_3$CN** have been determined by X-ray diffraction. Upon excitation at λ > 380 nm, the solid samples of complexes **3a**–**3d** show orange light at 298 K. Anion binding properties of complexes **3a**–**3d** have been studied by UV–vis titration experiments in CH_3CN and DMSO. In general, the log *K* values of **3a**–**3d** with the same anion in CH_3CN depend on the substituent R on the acetylide ligand of **3a**–**3d** and follow this order: R = NO_2 (**3d**) > CF_3 (**3c**) > Cl (**3b**) > H (**3a**). For the same complex with different anions, the log *K* values are in the following order: F^- > OAc^- > Cl^- > Br^- ≈ HSO_4^- ≈ NO_3^- > I^-, which is in line with the decrease of the basicity of anions. Complex **3d** with NO_2 group shows the dramatic colour change towards F^- in DMSO, providing the access of naked eye detection of F^-.

Introduction

Anion sensors have attracted consecutive interests over the past decade because of the crucial importance of anions and their potential applications in chemistry, biology as well as environment.[1] Since the pioneering work of Park and Simmons on the first anion sensor,[2] a variety of artificial anion receptors have been designed and synthesized for the stimulation of host-guest interactions within the supramolecular chemistry. Thus, much effort has been devoted to the exploitation of selective anion sensors. An ideal anion sensor consists of a receptor center for binding anions which is covalently linked to a reporting center for signaling of interaction.[3] Sensing signal was generated once the receptor center binds anions through non-covalent interactions, and the binding of such species could produce change in photophysical and redox properties of the reporter unit. Urea,[4, 5] thiourea,[5] amide,[6] and guandinium[7] based organic compounds were reported as anion sensors due to their specific hydrogen bonding interaction towards anions. Among them, urea-based receptors have been extensively studied owing to their unique geometry (two hydrogen bonds towards anions) and their easy modification through organic synthesis.[4]

While the early studies mainly focused on the organic anion sensors,[8] metal complexes based anion sensors have also gained immense attention. Metal complexes could have some intrinsic properties, such as redox and luminescence, and the metal center could directly interact with anions. Thus, anion recognition and sensing by metal complexes are supposed to extend the detection of anion binding. Iron(II),[9] rhenium(I),[10] ruthenium(II),[11] iridium,[12] gold(I),[13] terbium(III),[14] and gold(I)-copper(I)[15] complexes with urea group have been reported as anion sensors. Amongst various metal complexes, a great deal of attention have been particularly given to the platinum(II) acetylide complexes because of their rich photoluminescence properties.[16] The square planar geometry of platinum(II) also allows the Pt ⋯ Pt interactions, which could affect the properties of electronic excited states. In this regard, platinum(II) acetylide complexes have been used as sensors for VOC,[17] pH,[18] ions,[19] temperature,[18a,20] and mechanical force.[17c,21] In addition, the charge transfer absorption in the visible region with corresponding higher quantum yield photoluminescence of platinum(II) acetylide complexes also facilitates the applications such as molecular recognition,[22] photocatalysts,[23] energy conversion materials,[24] electroluminescence[25] as well as broadband nonlinear transmission materials.[26] However, to the best of our knowledge, the study of anion-sensing properties of platinum(II) acetylide complexes has been less explored.[27]

Our group has a long-term interest in the study of the relationship between the structures and anion-binding properties of metal complexes.[13a,13b] To extend our study, in this paper, we have synthesized a series of platinum(II) acetylide complexes with urea group [Pt(^{t}Bu$_3$tpy)(C≡CC$_6$H$_4$-4-NHC(O)NHC$_6$H$_5$-R)](OTf) (^{t}Bu$_3$tpy = 4,4′,4″-tri-*tert*-butyl-2,2′:6′,2″-terpyridine; R = H (**3a**), Cl (**3b**), CF_3 (**3c**), NO_2 (**3d**); Scheme 1). Their photophysical and anion-binding properties have been investigated. We envisaged that if the photophysical properties of these platinum(II) acetylide complexes could be changed when they interact with anions through hydrogen bonds between the

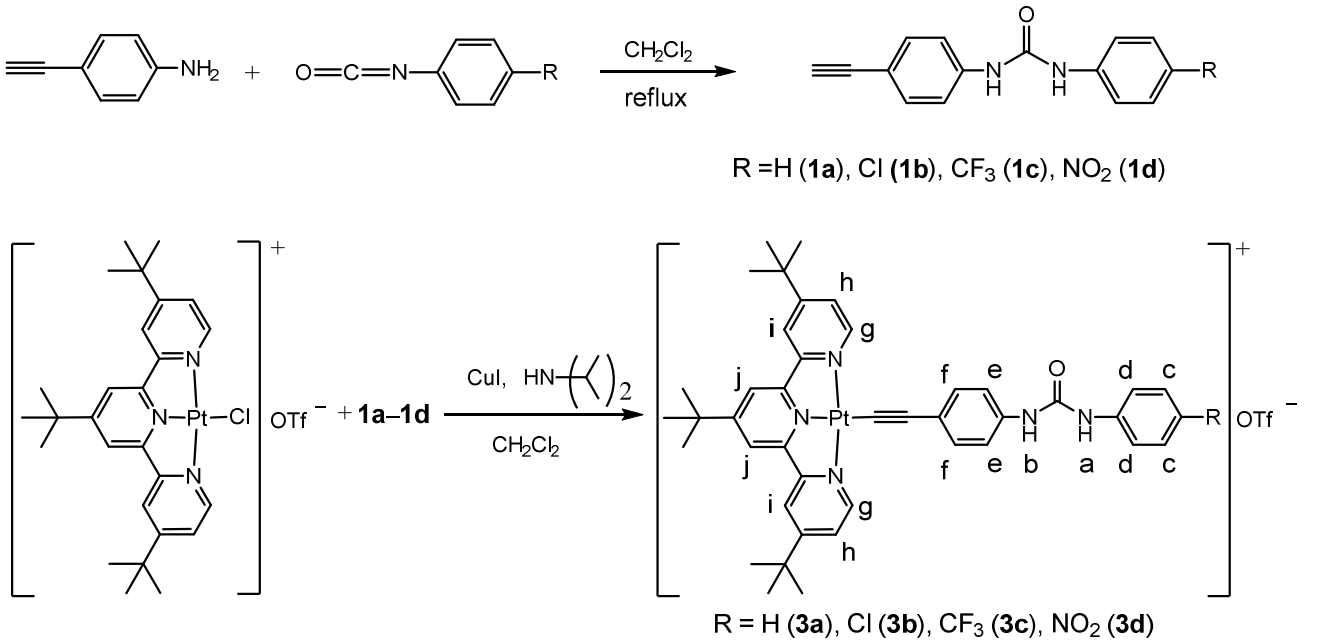

Scheme 1. Synthetic route of platinum(II) acetylide complexes **3a–3d**

urea N−H(s) of the complexes and anions, they could be used as anion sensors. In addition, the effect of the substituent R on the acetylide ligand on the anion-binding ability of the complexes **3a**–**3d** has also been examined. Interestingly, complex **3d** show significant colour change when it interacted towards F^- in DMSO, providing the naked eye detection of F^-.

Results and discussion

Synthesis and characterization

Scheme 1 shows the synthetic routes of the acetylide ligands (**1a**–**1d**) and platinum(II) acetylide complexes (**3a**–**3d**). The acetylide ligands, HC≡CC_6H_4-4-NHC(O)NHC_6H_4-4-R (R = H (**1a**), Cl (**1b**), CF_3 (**1c**), NO_2(**1d**)), were prepared by the reaction of 4-ethynylaniline with the corresponding isocynate in a molar ratio of 1:1 in refluxing dichloromethane. Further reactions of [Pt(^{t}Bu$_3$tpy)Cl](OTf) (**2**) (^{t}Bu$_3$tpy = 4,4′,4″-tri-*tert*-butyl-2,2′:6′,2″-terpyridine) with **1a**–**1d** in the presence of CuI and diisopropylamine in dichloromethane gave **3a**–**3d**, respectively. All platinum(II) acetylide complexes **3a**–**3d** were characterized by ^{1}H NMR, IR as well as ESI-MS and gave satisfactory elemental analyses. They are all air-stable in the solid state at 298 K.

In the ^{1}H NMR spectra of the platinum(II) acetylide complexes **3a**–**3d** in DMSO-d_6, the protons of N–H on the acetylide ligands of the complexes show the resonance at *ca.* 8.65–9.46 ppm. These chemical shifts are in the following order: **3a** < **3b** < **3c** < **3d**, which is in the line with the increasing of the electron-withdrawing ability of the substituent R on the acetylide ligand. In addition, the chemical shifts at *ca.* 6.96–8.18 ppm are attributed to the resonance of the protons on the aromatic rings of the acetylide ligand. The chemical shifts at *ca.* 7.85–9.02 ppm as well as 1.43 and 1.53 ppm are attributed to the resonance of the protons on the ^{t}Bu$_3$tpy ligand. The IR spectra of **3a**–**3d** reveal the bands at 3350−3433 and 1610−1641 cm^{-1}, characteristic of ν(N−H) and ν(C=O) of the acetylide ligands, respectively.

Crystal Structures of 3a, 3a·DMF·THF, 3b·CH_3CN, and 3c·CH_3CN

The crystal structure of the platinum(II) acetylide complexes **3a**, **3a·DMF·THF**, **3b·CH_3CN**, and **3c·CH_3CN** have been determined by X-ray diffraction. Their crystallographic data as well as selected bond distances and angles are listed in Table S1 (ESI†) and Table 1, respectively. Fig. 1 shows the perspective view of **3a** (for **3a·DMF·THF**, **3b·CH_3CN**, and **3c·CH_3CN**, see Fig. S2–S4 (ESI†). The platinum(II) coordination geometry in these complexes is distorted square-planar. The Pt–N bond distances are in the range of 1.949(5)–2.029(5) Å, which are similar to those of other related platinum(II) acetylide complexes.[22c,27d,28] The Pt1–C1 and C1≡C2 bond distances are 1.966(8)–1.992(8) and 1.206(10)–1.219(10) Å, respectively, which are comparable to those of other related platinum(II) acetylide complexes.[27d,28] The N1–Pt1–N2, N2–Pt1–N3, and N1–Pt1–N3 angles are *ca.* 80°, 80°, and 160°, respectively, which could be due to the geometric constraints of the ^{t}Bu$_3$tpy ligand. Each pair of complex cations reveals a head-to-tail stacking with the shortest Pt···Pt distance of *ca.* 4.931–9.253 Å. In addition, there is hydrogen bond interaction between the N–H of the urea group on the acetylide ligand and the oxygen atom of the triflate anion. The hydrogen bond parameters are listed in Table S2 (ESI†).

Table 1. Selected bond distances (Å) and bond angles (°) of complexes **3a**, **3a·DMF·THF**, **3b·CH_3CN**, and **3c·CH_3CN**

	3a	**3a·DMF·THF**	**3b·CH_3CN**	**3c·CH_3CN**
Pt···Pt (shortest)	5.804	9.253	4.931	5.139
Pt1–N1	2.027(6)	2.020(4)	2.029(5)	2.027(3)
Pt1–N2	1.956(6)	1.949(5)	1.973(6)	1.960(3)
Pt1–N3	2.026(6)	2.015(4)	2.022(5)	2.017(3)
Pt1–C1	1.967(7)	1.966(8)	1.992(8)	1.971(5)
C1–C2	1.219(10)	1.213(10)	1.206(10)	1.210(7)
C36–O1	1.154(13)	1.219(8)	1.225(7)	1.208(6)
N1–Pt1–N2	80.2(2)	80.08(17)	80.39(19)	80.41(13)
N2–Pt1–N3	80.6(2)	80.66(17)	80.41(17)	80.46(13)
N1–Pt1–N3	160.7(2)	160.63(18)	160.79(19)	160.87(13)
N1–Pt1–C1	100.6(3)	99.9(2)	98.6(2)	98.82(15)
N2–Pt1–C1	178.4(3)	179.6(2)	179.0(2)	179.12(16)
N3–Pt1–C1	98.6(3)	99.4(2)	100.6(2)	100.32(15)
Pt1–C1–C2	176.0(6)	177.3(7)	177.0(5)	176.8(4)

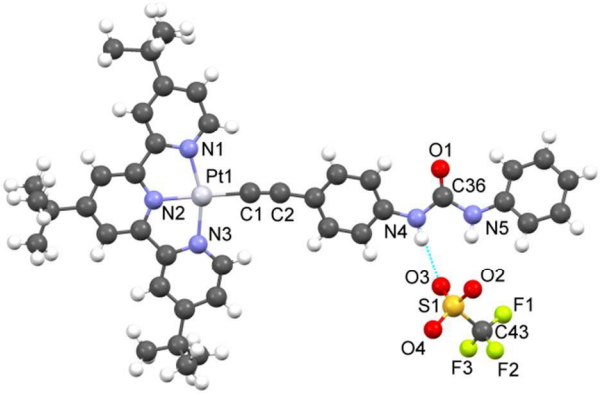

Fig. 1. Perspective view of **3a.**

Fig. 2 shows the stacking patterns of adjacent planar platinum(II) moieties as well as the arrangement for complexes **3a**, **3a·DMF·THF**, **3b·CH_3CN**, and **3c·CH_3CN**. These platinum(II) acetylide complexes with different acetylide ligands tend to pack in diverse arrangements. Their adjacent platinum(II) moieties display an antiparallel stacking pattern. Fig. 2(a) shows the molecular packing of **3a**, in which the adjacent Pt atoms are in the zigzag arrangement with a Pt···Pt···Pt angle of 170.39° and the Pt···Pt distance alternates between 5.804 and 8.575 Å. In addition, no significant Pt···Pt or π···π interaction is observed from the crystal packing due to the bulky *tert*-butyl groups on the terpyridyl ligands, which prevent the neighboring molecules from forming close proximity with each other. While viewed along the c axis, the platinum atoms are almost superimposable to give a zigzag $[Pt]_n$ chain. The individual molecules in the dimers are rotated with respect to their neighbors, with a C–Pt–Pt–C torsion angle of 180° and a partial stacking of the aromatic terpyridyl units. Unlike **3a**, where the Pt metal center shows a strong propensity to form a zigzag chains with shorter intermolecular Pt···Pt contacts, the molecular packing in **3a·DMF·THF** exhibits a farther distance between adjoining platinum atoms caused by the insert of solvent molecules into the lattice, giving two kinds of Pt···Pt distances to form a hexagon (Fig. 2(b)). The adjacent Pt···Pt distance is 9.253 Å between the platinum atoms arranged in the same order, while for those head-to-tail arrangement platinum atoms, the nearest Pt···Pt distance is 9.841 Å. The view along the c axis shows the platinum atoms are arranged in a honeycomb lattice. The THF molecule are inserted into the lattice through the three C–H···O hydrogen bonds (d (H···O1) = 2.667 Å, ∠(C–H···O1) = 171.25°; d(H···O2) = 2.528 Å, ∠(C–H···O2) = 173.36°; d(H···O3) = 2.618 Å, ∠(C–H···O3) = 153.56°), whereas the DMF molecule forms two C–H···O hydrogen bonds with two hydrogen atoms of pyridine ring (d(H···O1) = 2.458Å, ∠(C–H···O1) = 156.73°, d(H···O2) = 2.588 Å, ∠(C–H···O2) = 162.30°). It is interesting to note that the stacking varies in **3a** with/without solvates. Such difference may indicate the aggregation of **3a** is solvate-dependent.

Fig. 2(c) shows the molecular packing of **3b·CH_3CN**, in which CH_3CN molecule are inserted into the lattice through the C–H···N interaction between the hydrogen atom on the pyridine ring and the nitrogen atom on the acetonitrile molecule (d (H···N) = 2.655 Å, ∠(C–H···N) = 128.50°). When viewed along the a axis, the adjacent Pt atoms form head-to-tail dimeric structure with the adjacent Pt···Pt distance alternates between 4.931 and 10.001 Å, giving a zigzag $[Pt]_n$ chain with a Pt–Pt–Pt angle of 159.16°. The shortest Pt···Pt distance is 4.931 Å, which is shorter than that of **3a**, while the distance between the Pt atoms of diverse adjacent dimeric unit is longer (10.001 Å). This could be due to the insertion of CH_3CN molecule into the cavity, through which the distance of neighboring dimeric units increases while the Pt···Pt distance in the dimeric Pt atoms decreases. The stacking pattern of **3c·CH_3CN** has the same orientation as that of **3b·CH_3CN** (Fig. 2(d)). Both of them exist as sequential dimeric units with no evidence of Pt···Pt contacts. The shortest Pt···Pt distance of **3c·CH_3CN** is 5.139 Å, which is farther than that of **3b·CH_3CN** (4.931 Å). However, the distance between the Pt atoms of nearby dimers decreases to 9.968 Å. Moreover, the Pt–Pt–Pt angle is 158.31° of zigzag $[Pt]_n$ chain when viewed from the c axis. Although the CH_3CN molecules are found in the crystal structure, there is no significant interaction between the solvent molecule CH_3CN and *tert*-butyl group. Crystal structures of **3b·CH_3CN** and **3c·CH_3CN** are another examples of solvent-dependent aggregation which may indicate the molecules tend to pack in the same aggregation in the same solvent.

(a)

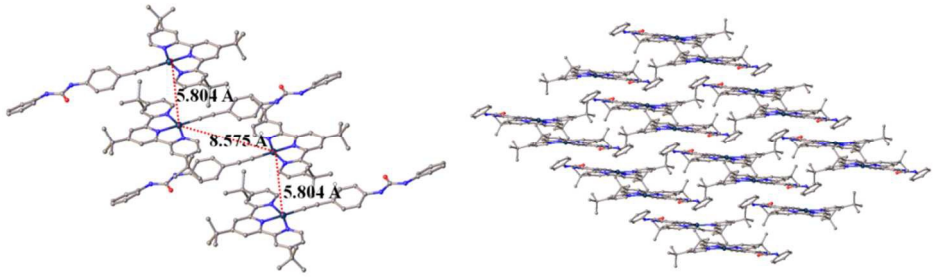

(b)

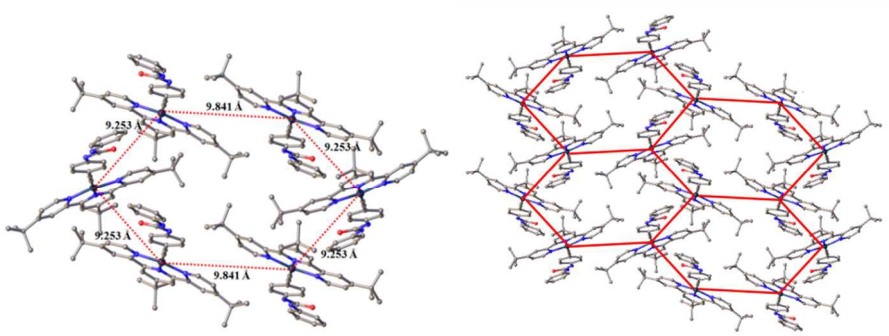

(c)

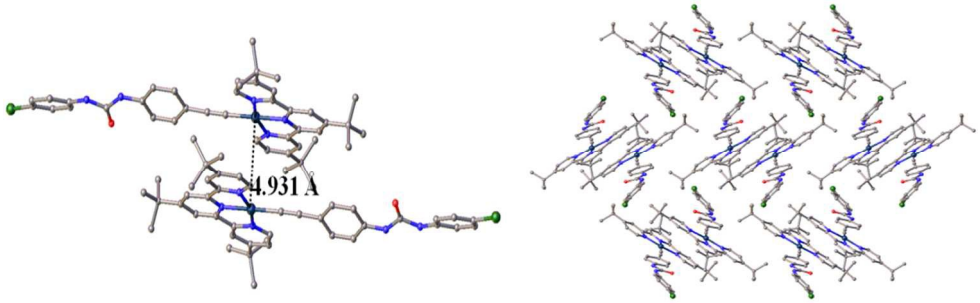

(d)

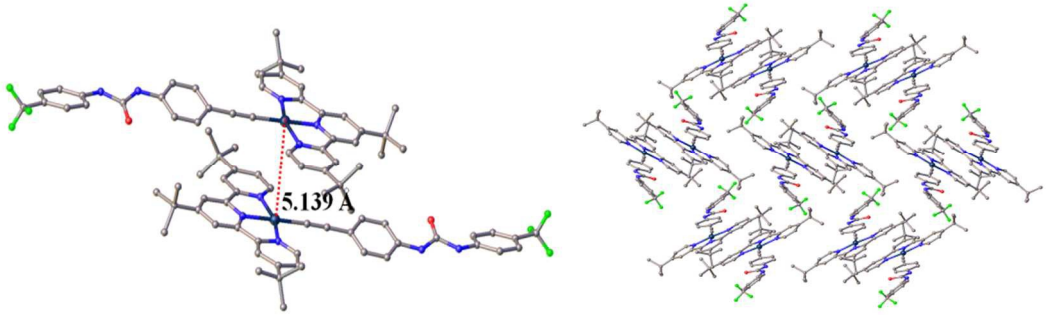

Fig. 2. Packing diagrams of (a) **3a**, (b) **3a**·**DMF**·**THF**, (c) **3b**·CH_3CN, and (d) **3c**·CH_3CN (left: stacking patterns of adjacent planar platinum(II) moieties; right: arrangement of the molecules; counter-anions are omitted for clarity)

Electronic absorption and emission spectra of complexes 3a–3d

The photophysical data for acetylide ligands (**1a–1d**) and complexes (**3a–3d**) are summarized in Table S3 (ESI†) and Table 2, respectively. The electronic absorption spectra of **3a–3c** in acetonitrile show the high-energy bands at 247–339 nm, which are assigned as the $\pi \rightarrow \pi^*$ transitions of the ^{t}Bu$_3$tpy and acetylide ligands (Fig. 3). For **3d** in acetonitrile, the electronic absorption bands at 312, 328, and 339 nm could be due to the charge transfer transition from the amide to the NO_2 group of the acetylide ligand.[13b] The low-energy bands of **3a–3d** in acetonitrile at 398–464 nm are ascribed to the admixture of MLCT (dπ(Pt) $\rightarrow$ π^*(^{t}Bu$_3$tpy)) and LLCT (π(C≡C-C$_6$H$_4$-NH-C(O)-NH-C$_6$H$_4$-4-R) $\rightarrow$ π^*(^{t}Bu$_3$tpy)) transitions. The ground-state complex aggregation of **3a** in DMSO has also been studied. When the concentration of **3a** in DMSO increases from 1×10^{-5} to 1×10^{-3} mol· dm^{-3}, the absorbance at 510 nm obeys Beer's law (Fig. S4 and S5, ESI†), suggesting that there is no aggregation of **3a** in DMSO in the concentration ranging from 10^{-5} to 10^{-3} mol· dm^{-3}. This result may be due to the steric effect from the bulky ^{t}Bu$_3$tpy ligand, preventing the aggregation of **3a**.[29]

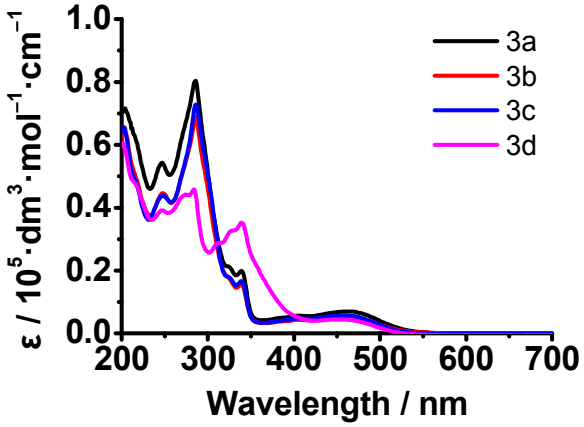

Fig. 3. Electronic absorption spectra of **3a–3d** in acetonitrile at 298 K

It is interesting to note that platinum(II) acetylide complexes **3a–3d** exhibit different colours in different solvents. Because **3a** has the better solubility in solvents, it has been used to study the solvent effect on the electronic absorption spectrum. Fig. 4(a) shows the colours of **3a** at the concentration of 2.7×10^{-5} mol·dm^{-3} in different solvents: light yellow (DMSO, CH_3CN, and CH_3OH), orange ($CH_3C(O)CH_3$), and pale red (CH_2Cl_2 and THF). Fig. 4(b) shows the electronic absorption spectra of **3a** in 370–700 nm in various solvents. The low-energy absorption maximum is in the order: CH_3OH (458 nm) < CH_3CN (464 nm) < DMSO (472 nm) < $CH_3C(O)CH_3$ (476 nm) < THF (492 nm) < CH_2Cl_2 (498 nm) depending on the solvent polarity (Table S4, ESI†). However, there is no clear trend between the absorption maximum and solvent polarity. Similar trend can also been observed in **3b** (Table S4 and Fig. S6, ESI†). The solvent-dependent absorption bands indicate their charge-transfer character in nature.

(a)

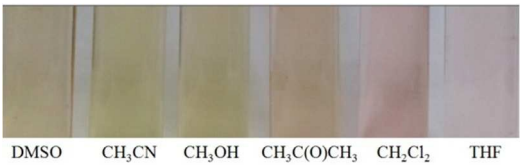

(b)

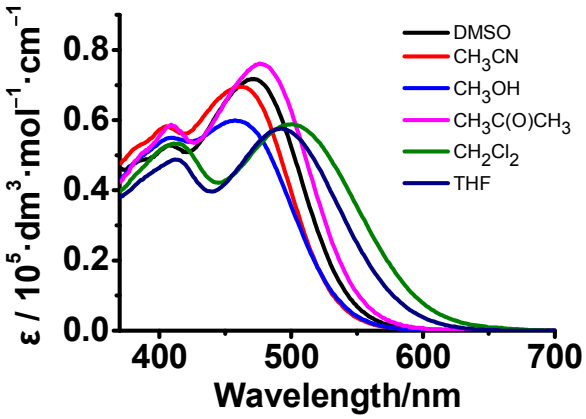

Fig. 4. (a) Colours of **3a** (concentration = 2.7×10^{-5} mol·dm^{-3}) in various solvents. (b) Electronic absorption spectra of **3a** in 370–700 nm in various solvents at 298 K.

Excitation of complexes **3a–3d** in the solid state at $\lambda > 380$ nm produces orange light. The emission maxima of **3a–3d** in the solid state at 298 K are in the order: 616 nm (**3a**) > 607 nm (**3b**) > 601 nm (**3c**) > 599 nm (**3d**), which is in line with the increasing of the electron-withdrawing ability of the substituent R on the acetylide ligand (R = H (**3a**) < Cl (**3b**) < CF_3 (**3c**) < NO_2 (**3d**)) (Fig. 5). The lifetime of these emission bands is 0.249–0.502 μs, indicating the nature of the triplet excited state. The stronger electron-withdrawing acetylide ligand could reduce the energy of dπ(Pt)- and π(acetylide ligand)-based HOMO.[26d] Thus, the emission band at 599–616 nm for **3a–3d** in the solid state is tentatively assigned to come from the mixture of ^{3}MLCT (dπ(Pt) $\rightarrow$ π^*(^{t}Bu$_3$tpy)) and ^{3}LLCT (π(acetylide ligand) $\rightarrow$ π^*(^{t}Bu$_3$tpy)) excited states. However, in solutions, complexes **3a–3d** show very weak or no emission at 298 K.

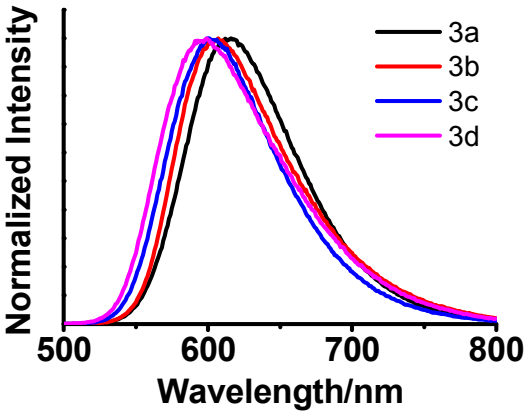

Fig. 5. Emission spectra of **3a–3d** in the solid state at 298 K

Table 2. Photophysical data of complexes **3a**–**3d** at 298 K

complex	medium	λ_{abs} / nm (ε / dm^3·mol^{-1}·cm^{-1})	λ_{em}/nm (τ_0/μs)[a]
3a	DMSO	247 (sh, 43150), 289 (61480), 329 (sh,16180), 344 (14300), 384 (sh, 4830), 407 (5290), 472 (7170)	
	CH_3CN	247(54280), 259 (sh, 51280), 285 (80320), 323 (sh,21320), 383 (sh, 5240), 405 (5820), 464 (6940)	
	THF	249 (41440), 287 (64960), 340 (sh, 14740), 388 (sh, 4330), 412 (4880), 492 (5760)	
	CH_2Cl_2	231 (39220), 251 (44550), 287 (67440), 338 (15890), 411 (5330), 498 (5870)	
	$CH_3C(O)CH_3$	328 (15960), 339 (16150), 389 (sh, 5130), 409 (5870), 476 (7610)	
	CH_3OH	249 (45070), 285 (73670), 325 (sh, 18630), 339 (17520), 382 (sh, 4830), 409 (5500), 458 (5990)	
	solid		616 (0.426)
3b	DMSO	260 (sh,40160), 290 (69350), 329 (sh,19880), 344 (16690), 404 (sh, 4430), 469 (5640)	
	CH_3CN	247 (39105), 285 (68455), 324 (sh,17720), 339 (15530), 403 (sh, 4310), 460 (5160)	
	THF	289 (41830), 340 (sh,3440), 413 (2670), 493 (3020)	
	CH_3OH	286 (80060), 326 (sh,18290), 339 (17770), 395 (sh, 5350), 453(6380)	
	CH_2Cl_2	287 (78500), 339 (17500), 412 (5240), 502 (5880)	
	solid		607 (0.345)
3c	DMSO	260 (sh, 41430), 291 (65140), 332 (sh, 15990), 344 (14180), 404 (sh, 4080), 469 (5610)	
	CH_3CN	247 (43850), 286 (72810), 324 (sh, 17950), 339 (16670), 402 (sh, 4670), 459 (5700)	
	solid		606 (0.249)
3d	DMSO	260 (sh, 42520), 285 (51520), 332 (sh, 30800), 346 (34320), 468 (7480)	
	CH_3CN	246 (39105), 273 (sh, 65760), 284 (45850), 312 (28780), 328 (32720), 339 (35280), 459 (4430)	
	solid		599 (0.502)

[a] The emission of **3a–3d** was too weak to be observed in these solvents.

Anion binding properties of complexes 3a–3d in CH_3CN

The binding properties of **3a**–**3d** in CH_3CN towards anions, such as F^-, Cl^-, Br^-, I^-, OAc^-, NO_3^-, HSO_4^-, SO_4^{2-}, and $H_2PO_4^-$ (used their tetra-*n*-butylammonium salts), have been investigated by the UV–vis titration experiments. Because the precipitates were produced during the titration of **3a**–**3d** with SO_4^{2-} and $H_2PO_4^-$, corresponding investigations were not carried out. Fig. 6 shows the UV–vis spectral changes of **3d** upon addition of F^- in CH_3CN at 298 K. The absorbance of the absorption bands of **3d** at 245, 271, 283, 311, 326, 340, and 453 nm decreases gradually, while the new absorption bands at 371 and 480 nm appear with the intensity increasing progressively. Consequently, the solution colour (5×10^{-5} mol·dm^{-3}) changes from pale yellow to light red. Well-defined isosbestic points are observed at 287, 301 and 358 nm, indicating that only two species coexist during the titration equilibrium and suggesting the possible formation of anion−complex adduct. Addition of other anions (Cl^-, Br^-, I^-, OAc^-, NO_3^-, and HSO_4^-) into the CH_3CN solution of **3d** causes similar (but smaller) spectral changes to those towards F^- (Fig. S7–S12, ESI†).

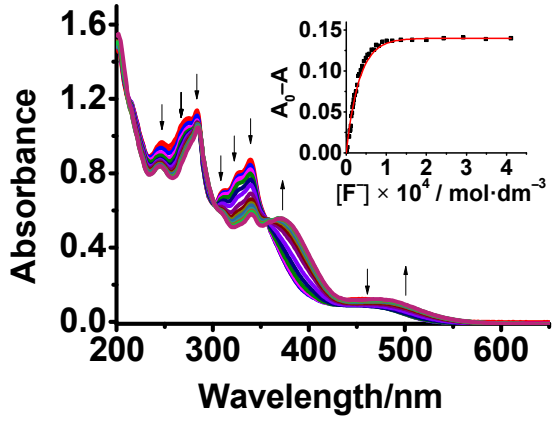

Fig. 6. UV–vis spectral changes of **3d** (5×10^{-5} mol·dm^{-3}) in CH_3CN upon addition of F^-. Insert: A plot of the absorbance change at 250 nm as a function of the concentration of F^- and its theoretical fit for the 1:1 binding of complex **3d** with F^-.

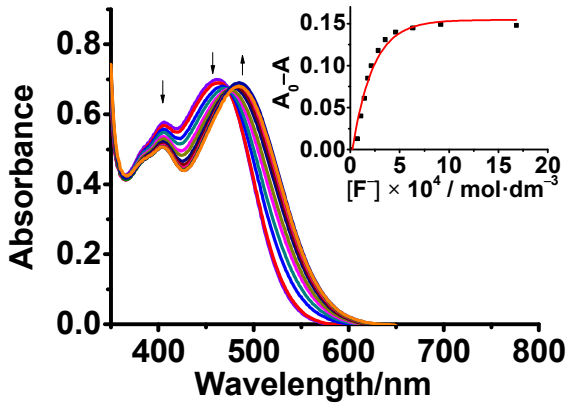

Fig. 7. UV–vis spectral changes of **3a** (1.2×10^{-4} mol·dm^{-3}) in CH_3CN upon addition of F^-. Insert: A plot of the absorbance change at 430 nm as a function of the concentration of F^- and its theoretical fit for the 1:1 binding of complex **3a** with F^-.

For non-nitro-derivatives **3a**–**3c**, their UV–vis spectral changes in CH_3CN are similar to each other upon addition of anions studied in this paper (Fig. S13–S32, ESI†). Fig. 7 demonstrates the UV–vis spectral changes of **3a** upon addition of F^- in CH_3CN at 298 K. During the process, the absorption bands at 405 and 461 nm decrease gradually, and a new band at 485 nm appears. A well-defined isosbestic point is observed at 473 nm. To determine the binding ratio between the complex and anion, the Job's plots have been made. Fig. S33(a) (ESI†) shows the Job's plots of complexes **3a**–**3d** with F^- in CH_3CN. The absorbance maximum appeares at *ca.* 0.5, indicating the 1:1 complex-anion formation. Using the 1:1 binding model and non-linear least-squares fitting, the log *K* values of **3a**–**3d** towards different anions were determined (Table 3). For complexes **3a**–**3d** with the same anion, their log *K* values are in the following order: R = NO_2 (**3d**) > CF_3 (**3c**) > Cl (**3b**) > H (**3a**), which is in line with the decreasing of the electron-withdrawing ability of the substituent R on the acetylide ligand of **3a**–**3d**. This result could be rationalized by the fact that the electron-withdrawing substituent R on the acetylide ligand of **3a**–**3d** would increase the acidity of urea N−H(s) and strengthen the hydrogen bond interactions between the urea N−H(s) of the complexes and anions. In addition, for the same

Table 3. Binding constants (log *K*) of **3a**–**3d** with anions in CH_3CN[a]

Complex	F^-	OAc^-	Cl^-	Br^-	I^-	NO_3^-	HSO_4^-
3a	4.52±0.14	4.34±0.16	3.35±0.02	2.53±0.03	[b]	2.31±0.06	2.63±0.08
3b	4.88±0.18	4.48±0.21	3.51±0.03	2.75±0.07	2.34±0.15	2.82±0.13	2.92±0.05
3c	5.07±0.51	4.96±0.13	3.80±0.06	2.92±0.05	2.48±0.06	2.90±0.14	3.02±0.13
3d	5.53±0.11	5.22±0.21	3.85±0.08	3.03±0.04	2.60±0.05	2.91±0.09	3.09±0.05

[a]Binding constants were determined by 1:1 model using nonlinear fitting methods. [b]Spectral changes were not suitable for accurate measurement of binding constant.

complex with different anions, the log *K* values are in the following order: $F^- > OAc^- > Cl^- > Br^- \approx HSO_4^- \approx NO_3^- > I^-$, which is in line with the decrease of the basicity of anions.

Anion binding abilities of complexes of 3a–3d towards F^- in DMSO

In our previous work on the anion sensing studies of gold(I) acetylide complexes,[13b] the deprotonation process of the N–H of urea group could be observed upon addition of F^- into the DMSO solution of gold(I) acetylide complex with nitro-group. To examine this phenomenon in the platinum(II) complex **3d**, the UV–vis and ^{1}H NMR titration experiments of **3d** towards F^- in DMSO and DMSO-d_6 have been done. Fig. 8(a) and 8(b) show the UV–vis spectral changes of **3d** in DMSO upon addition of F^- at 298 K. When 0–9 equivalents of F^- are added, the absorbance of the absorption bands at 285, 330, as well as 347 nm decreases gradually while the absorbance at 379 and 489 nm increases. Well-defined isosbestic points are observed at 308 and 371 nm (Fig. 8(a)). After more than 9 equivalents of F^- were added, well-defined isosbestic points are observed at 296, 326 and 420 nm and the absorbance of the band at 489 nm increases remarkably (Fig. 8(b)). Thus, the solution colour of **3d** gradually alters from yellow to red. We propose two processes occur upon addition of F^- into the DMSO solution of **3d**. The first one is the hydrogen bond interaction between the urea N–H(s) of **3d** and F^-, which occurs at low concentrations of F^-. The second one is the deprotonation of the urea N–H of **3d** when the concentration of F^- is high. The appearance of the low-energy absorption band at 489 nm is ascribed to the deprotonation of the urea N–H of **3d** (*vide infra*). On the contrary, by stepwise addition of F^- into **3a**–**3c** in DMSO (Fig. S34–S36, ESI†), the colour changes from yellow to orange and UV–vis spectral changes are similar to those of **3a**–**3c** with F^- in CH_3CN (Fig. S13, S19, and S26, ESI†, respectively). The binding constants of **3a**–**3c** with F^- in DMSO are smaller than those in CH_3CN (Table S5, ESI†). This result could be rationalized by the fact that the DMSO solvent could compete with F^- to form hydrogen bonds with urea group of **3a**–**3c** and reduce the binding abilities of **3a**–**3c** towards F^-. The UV–vis spectral changes of **3d** towards OAc^- in DMSO (Fig. S37, ESI†) are different from those of **3d** towards F^- and are similar to those of **3d** towards OAc^- in CH_3CN; the colour of the solution changes from yellow to orange. Moreover, addition of other anions (Cl^-, Br^-, NO_3^-, and HSO_4^-) into the DMSO solution of **3d** causes little spectral change (Fig. S38–S41, ESI†, respectively). For **3a**–**3c**, addition of OAc^- can cause a little spectral changes but addition of Cl^-, Br^-, NO_3^-, and HSO_4^- produces little spectral change in the DMSO solution (Fig. S42–S55, ESI†).

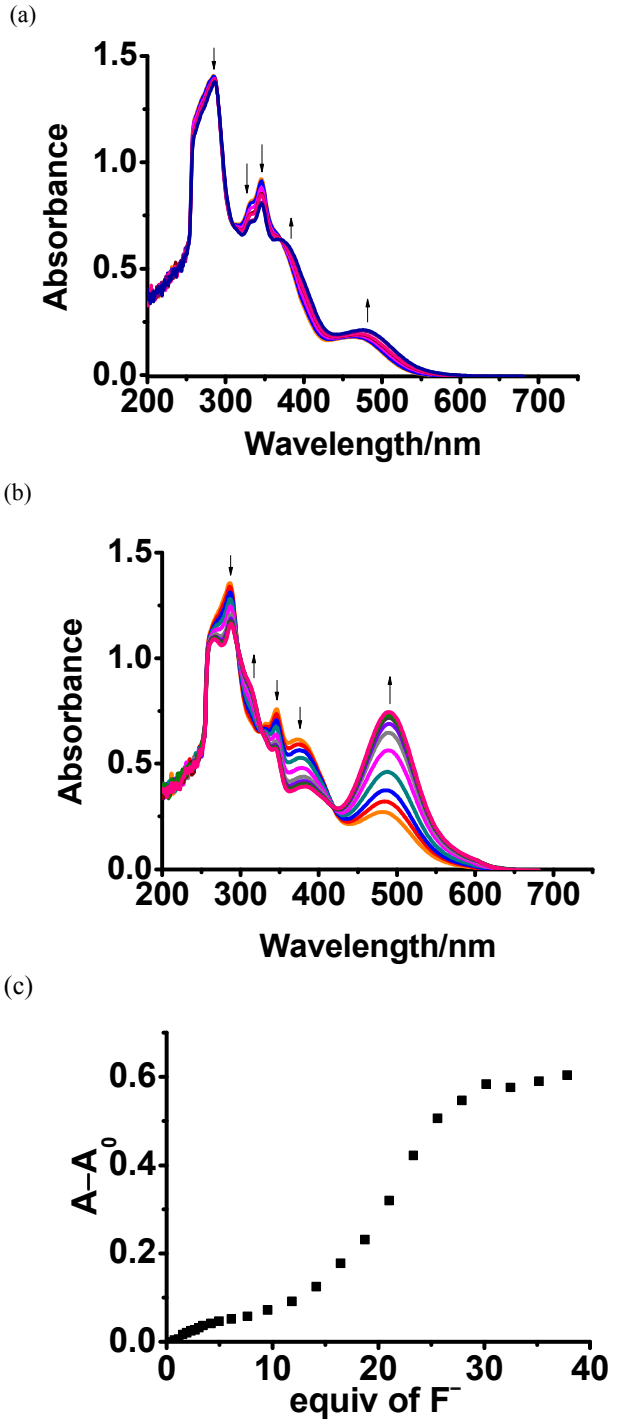

Fig. 8. UV–vis spectral changes of **3d** (3×10^{-5} mol·dm^{-3}) in DMSO upon addition of F^-: (a) 0-9 equiv, (b) 9-13 equiv; (c) A plot of the absorbance change at 489 nm as a function of the concentration of F^-

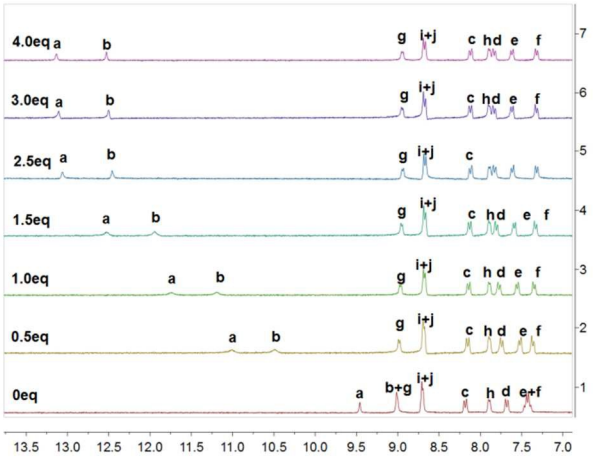

Fig. 9. ^{1}H NMR spectral changes of **3d** upon addition of OAc^- in DMSO-d_6

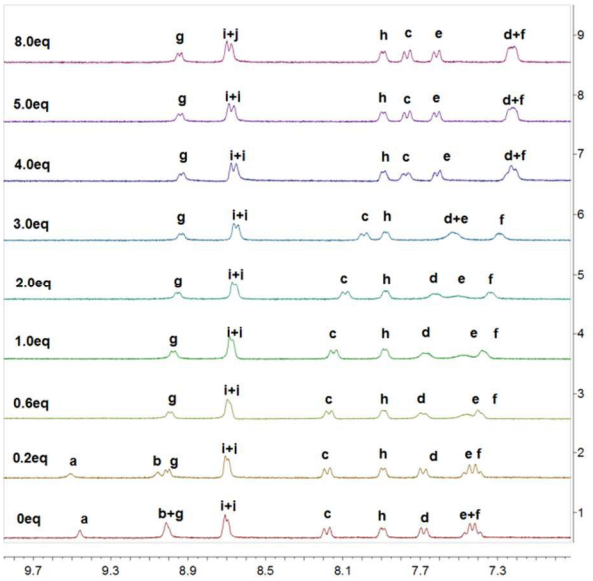

Fig. 10. ^{1}H NMR spectral changes of 3d upon addition of F^- in DMSO-d_6 at 6.90-9.85 ppm

The ^{1}H NMR titrations experiments of **3d** with F^- and OAc^- have also been investigated. Fig. 9 shows the spectral changes of **3d** upon addition of OAc^- in DMSO-d_6. Obvious downfield shift of urea N−H (H_a and H_b) is found upon addition of OAc^- from 0 to 2.5 equiv. Further addition after 3.0 equiv does not cause any spectral change. This result indicates there are hydrogen bond interactions between the urea N−Hs of **3d** and the acetate anion. The signals of H_{c-g} undergo a little upfield or downfield shift upon addition of OAc^- from 0 to 4.0 equiv, which may be due to the through-bond propagation or through-space effect, respectively.[30] Fig. 10 shows the ^{1}H NMR spectral changes of **3d** upon addition of F^- in DMSO-d_6. Upon addition of 0.2 equiv of F^- into the DMSO-d_6 solution of **3d**, the signals of the urea protons (H_a and H_b) disappear and the signals of H_{c-f} show a little shift. After 4 equiv of F^- is added, a triplet centred at 16.10 ppm (J = 120 Hz), which is assigned as the signal of HF_2^-, appears (Fig. S56, ESI†). The signals of H_{c-f} on the acetylide ligand exhibit little shift when the amount of F^- added is less than 2 equiv. Upon addition of more than 2 equiv of F^-, H_c, H_d, and H_f show the dramatic upfield shift, which could be due to the enhancement of shielding effect resulting from the increased electron density of aromatic ring through the increased through-bond negative charge delocalization that caused by the deprotonation process of urea N–H on the acetyllide ligand.[29d] In the ^{19}F NMR spectra, when the addition of F^- into the DMSO-d_6 solution of **3d** is larger than 3 equiv, a doublet centred at −142.5 ppm (J = 129 Hz) is observed, suggesting the formation of HF_2^- (Fig. S57, ESI†). This result also supports the deprotonation process of the urea N–H of **3d** in DMSO-d_6.

Conclusion

Platinum(II) acetylide complexes bearing urea group **3a–3d** have been synthesized and characterized. These complexes show orange light emission in the solid state at 298 K, which is assigned to come from the ^{3}MLCT/^{3}LLCT excited states. In CH_3CN, the anion-binding constant (log K) of this class of complexes towards the same anion depends on the substituent R on the acetylide ligand of 3a–3d: R = NO_2 (**3d**) > CF_3 (**3c**) > Cl (**3b**) > H (**3a**). In addition, for the same complex with different anions, the log K values follow this order: $F^- > OAc^- > Cl^- > Br^- \approx HSO_4^- \approx NO_3^- > I^-$. In DMSO, 3d shows the selective colour change towards F^-, and this is ascribed to the deprotonation of urea N−H of the acetylide ligand of **3d**. The solvent-dependent and selective colour change of **3d** towards F^- provides access for naked eye detection of F^-.

Experimental

Materials and reagents

[Pt(^{t}Bu$_3$tpy)Cl](OTf) (**2**) was synthesized according to the literature procedure.[31] 4-Ethynylaniline was obtained from Acros. 4-Chlorophenyl isocyanate, K_2PtCl_4, $LiClO_4$ and $LiSO_3CF_3$ were obtained from Energy Chemical. 4-Trifluoromethyl isocyanate, and 4-nitrophenyl isocyanate were obtained from J&K. 4,4′,4″-Tri-*tert*-butyl-2,2′:6′,2″-terpyridine was obtained from Sigma-Aldrich. The solvents were dried and distilled, prior to use except that those for spectroscopic measurements were of spectroscopic grade. Other reagents were purchased from commercial sources and used as received unless stated otherwise. All reactions were carried out under anhydrous and anaerobic conditions using standard Schlenk techniques under nitrogen.

Synthesis

HC≡CC$_6$H$_4$-4-NHC(O)NHC$_6$H$_5$ (1a)

A mixture of 4-ethynylaniline (300 mg, 2.56 mmol) and isocyanatobenzene (391 mg, 2.54 mmol) in dichloromethane (30 mL) was refluxed for 24 h under N_2. The yellow precipitate was collected and washed with dichloromethane and diethyl ether. Yield: 555 mg, 80 %. ^{1}H NMR (300 MHz, DMSO-d_6, 298 K) δ = 8.85 (s, 1H, NH), 8.70 (s,1H, NH), 7.43 (t, J = 7.0 Hz, 4H, aromatic ring), 7.76–7.35 (m, 6H, aromatic ring), 7.26 (t, J = 8 Hz, 2H, aromatic ring), 6.96 (s, 1H, aromatic ring), 4.03 (s, 1H, HC≡C). IR (KBr, cm^{-1}): ν = 3293 (N−H), 1627 (C=O). Anal. calcd for $C_{15}H_{12}N_2O$: C, 76.25; H, 5.12; N, 11.86 %. Found: C,

76.55; H, 5.08; N, 11.67%.

HC≡CC$_6$H$_4$-4-NHC(O)NHC$_6$H$_4$-4-Cl (1b)

The procedure was similar to that of complex **1a**, except 4-chlorophenyl isocyanate was used instead of isocyanatobenzene. Yield: 540 mg, 78 %. ^{1}H NMR (300 MHz, DMSO-d_6, 298 K) δ = 8.90 (s, 1H, NH), 8.86 (s,1H, NH), 7.47–7.38 (m, 4H, aromatic ring), 7.35–7.29 (m, 4H, aromatic ring), 4.04 (s, 1H, HC≡C). IR (KBr, cm^{-1}): ν = 3281 (N−H), 1641 (C=O). Anal. calcd for $C_{15}H_{11}ClN_2O$: C, 66.55; H, 4.10; N, 13.09 %. Found: C, 66.38; H, 4.12; N, 13.01%.

HC≡CC$_6$H$_4$-4-NHC(O)NHC$_6$H$_4$-4-CF$_3$ (1c)

The procedure was similar to that of complex **1a**, except 4-trifluoromethyl isocyanate was used instead of isocyanatobenzene. Yield: 466 mg, 72 %. ^{1}H NMR (300 MHz, DMSO-d_6, 298 K) δ = 9.14 (s, 1H, NH), 9.00 (s,1H, NH), 7.62 (s, 4H, aromatic ring), 7.46 (d, J = 9 Hz, 2H, aromatic ring), 7.38 (d, J = 9 Hz, 2H, aromatic ring), 4.05 (s, 1H, HC≡C). IR (KBr, cm^{-1}): ν = 3321 (N−H), 1647 (C=O). Anal. calcd for $C_{16}H_{11}F_3N_2O$: C, 63.16; H, 3.64; N, 9.21 %. Found: C, 62.98; H, 3.63; N, 9.11%.

HC≡CC$_6$H$_4$-4-NHC(O)NHC$_6$H$_4$-4-NO$_2$ (1d)

The procedure was similar to that of complex **1a**, except 4-nitrophenyl isocyanate was used instead of isocyanatobenzene. Yield: 166 mg, 46 %. ^{1}H NMR (300 MHz, DMSO-d_6, 298 K) δ = 9.46 (s, 1H, NH), 9.10 (s,1H, NH), 8.18 (d, J = 9 Hz, 2H, aromatic ring), 7.67 (d, J = 9 Hz, 2H, aromatic ring), 7.48 (d, J = 9 Hz, 2H, aromatic ring), 7.40 (d, J = 8.6 Hz, 2H, aromatic ring), 4.06 (s, 1H, HC≡C). IR (KBr, cm^{-1}): ν = 3290 (N−H), 1641 (C=O). Anal. calcd for $C_{15}H_{11}N_3O_3$: C, 64.05; H, 3.94; N, 14.94 %. Found: C, 63.98; H, 3.93; N, 14.94%.

[Pt(^{t}Bu$_3$tpy)(C≡CC$_6$H$_4$-4-NHC(O)NHC$_6$H$_5$)(OTf) (3a)

A mixture of 2 (70 mg, 0.088 mmol), **1a** (24 mg, 0.089 mmol), CuI (5 mg, 0.026 mmol), and diisopropylamine (1 mL) in dichloromethane (25 mL) was stirred for 18 h at room temperature. The orange precipitate was collected and washed with diethyl ether. The product was recrystallized from acetonitrile. Yield: 69 mg, 80 %. ^{1}H NMR (300 MHz, DMSO-d_6, 298 K) δ = 8.89 (d, J = 7 Hz, 2H, tpy), 8.74 (s, 1H, NH), 8.66–8.65 (m, 5H, tpy + NH), 7.85 (dd, J = 6 Hz, 2 Hz, 2H, tpy), 7.48–7.40 (m, 4H, aromatic ring), 7.42–7.35 (m, 2H, aromatic ring), 7.27 (t, J = 8 Hz, 2H, aromatic ring), 6.96 (t, J = 8 Hz, 1H, aromatic ring), 1.52 (s, 9H, ^{t}Bu), 1.43 (s, 18H, ^{t}Bu). IR (KBr, cm^{-1}): ν = 3420 (N−H), 1612 (C=O). ESI-MS: m/z = 832 [M – OTf]$^+$. Anal. calcd for $C_{43}H_{46}F_3N_5O_4PtS$: C, 52.65; H, 4.75; N, 7.14%. Found: C, 52.61; H, 4.76; N, 7.13%.

[Pt(^{t}Bu$_3$tpy)(C≡CC$_6$H$_4$-4-NHC(O)NHC$_6$H$_4$-4-Cl)(OTf) (3b)

The procedure was similar to that of complex **3a**, except **1b** was used instead of **1a**. Yield: 45 mg, 59 %. ^{1}H NMR (300 MHz, DMSO-d_6, 298 K) δ= 9.02 (d, J = 7 Hz, 2H, tpy), 8.85 (s, 1H, NH), 8.81 (s, 1H, NH), 8.71–8.70 (m, 4H, tpy), 7.90 (dd, J = 6 Hz, 2Hz, 2H, tpy), 7.49–7.30 (m, 8H, aromatic ring), 1.52 (s, 9H, ^{t}Bu), 1.43 (s, 18H, ^{t}Bu). IR (KBr, cm^{-1}): ν = 3356 (N−H), 1641 (C=O). ESI-MS: m/z = 866 [M – OTf]$^+$. Anal. calcd for $C_{43}H_{45}ClF_3N_5O_4PtS$: C, 50.86; H, 4.47; N, 6.90%. Found: C, 50.87; H, 4.46; N, 6.86%.

[Pt(^{t}Bu$_3$tpy)(C≡CC$_6$H$_4$-4-NHC(O)NHC$_6$H$_4$-4-CF$_3$)(OTf) (3c)

The procedure was similar to that of complex **3a**, except **1c** was used instead of **1a**. Yield: 55 mg, 63 %. ^{1}H NMR (300 MHz, DMSO-d_6, 298 K) δ = 9.17 (s, 1H, NH), 8.94 (s, br, 3H, tpy + NH), 8.69–8.65 (m, 4H, tpy), 7.87 (dd, J = 6 Hz, 2Hz, 2H, tpy), 7.66–7.64 (m, 4H, aromatic ring), 7.45 (d, J = 8.9 Hz, 2H, aromatic ring), 7.38 (d, J = 8.6 Hz, 2H, aromatic ring), 1.52 (s, 9H, ^{t}Bu), 1.43 (s, 18H, ^{t}Bu). IR (KBr, cm^{-1}): ν = 3433 (N−H), 1610 (C=O). ESI-MS: m/z = 900 [M – OTf]$^+$. Anal. calcd for $C_{44}H_{45}F_6N_5O_4PtS$: C, 50.38; H, 4.32; N, 6.68%. Found: C, 50.40; H, 4.30; N, 6.67%.

[Pt(^{t}Bu$_3$tpy)(C≡CC$_6$H$_4$-4-NHC(O)NHC$_6$H$_4$-4-NO$_2$)(OTf) (3d)

The procedure was similar to that of complex **3a**, except **1d** was used instead of **1a**. Yield: 50 mg, 70 %. ^{1}H NMR (300 MHz, DMSO-d_6, 298 K) δ = 9.46 (s, 1H, NH), 9.01 (s, br, 3H, tpy + NH), 8.71–8.69 (m, 4H, tpy), 8.18 (d, J = 9 Hz, 2H, aromatic ring), 7.89 (dd, J = 6 Hz, 2Hz, 2H, tpy), 7.68 (d, J = 9 Hz, 2H, aromatic ring), 7.47–7.39 (m, 4H, aromatic ring), 1.53 (s, 9H, ^{t}Bu), 1.44 (s, 18H, ^{t}Bu). IR (KBr, cm^{-1}): ν = 3350 (N−H), 2054 (C≡C), 1620 (C=O). ESI-MS: m/z = 877 [M – OTf]$^+$. Anal. calcd for $C_{43}H_{45}F_3N_6O_6PtS$: C, 50.34; H, 4.42; N, 8.19%. Found: C, 50.06; H, 4.48; N, 8.27%.

Measurements and instrumentation

Electronic absorption spectra were measured on a PGENERAL TU1901 UV−vis spectrophotometer. Emission spectra were obtained on a FLSP920 fluorescence spectrophotometer. Chemical shifts (δ, ppm) were reported relative to tetramethylsilane for ^{1}H NMR and NaF (δ = –122.4 ppm) for ^{19}F NMR on a Varian Mercury–Plus 300 spectrometer. Infrared spectra were recorded from KBr pellets in the range 400−4000 cm^{-1} on a Bruker-EQUINOX 55 FT-IR spectrometer. Electrospray ionization (ESI) mass spectra were recorded on a LCQ DECA XP quadrupole ion trap mass spectrometer. Elemental analysis was performed on an Elementar Vario EL elemental analyzer.

Crystal structure determination

Crystals of **3a**, **3b·CH$_3$CN**, and **3c·CH$_3$CN** were grown by diffusion of diethyl ether into DMF/MeOH (v/v = 1), DMF/CH$_3$CN (v/v = 1), and DMF/CH$_3$CN (v/v = 1) solutions, respectively. Crystals of **3a·DMF·THF** were obtained by layering diethyl ether onto DMF/THF (v/v = 1) solution. Selected single crystals of **3b·CH$_3$CN** and **3c·CH$_3$CN** were used for data collection on a Rigaku R–AXIS Spider IP with graphite monochromatized Mo–Kα radiation (λ = 0.71073 Å) and Cu–Kα (λ = 1.54178 Å) respectively, while **3a** and **3a·DMF·THF** were obtained by Oxford Gemini S Ultra CCD area detector diffractometer with graphite monochromatized Mo–Kα radiation (λ = 0.71073 Å). An empirical absorption correction was applied using the PROCESS-AUTO (Rigaku, 1998) or CrysAlisPro (Version 1.171.36.32) program. The structures were solved by direct methods and refined by the full-matrix least-square method based on F^2 with the program SHELXL-2013 using the OLEX2 software package.[32] In **3a**, large regions of diffuse electron density that can not be modeled (disordered solvents) were removed from the refinement, using SQUEEZE function in PLATON (See cif for details). CCDC 1028565, 1028514, 1028592, and 1028516 contain the supplementary

crystallographic data for **3a**, **3a·DMF·THF**, **3b·CH_3CN**, and **3c·CH_3CN**, respectively. These data can be obtained free of charge via http://www.ccdc.cam.ac.uk/conts/retrieving.html, or from the Cambridge Crystallographic Data Center, 12 Union Road, Cambridge CB2 1EZ, UK; fax: (+44) 1223 336-033; or e-mail: deposit@ccdc.cam.ac.uk.

Titrations and Job's plot

For a typical UV−vis titration experiment of **3a–3d** in CH_3CN, 0.2 μL aliquots of a tetra-*n*-butylammonium salt (concentrations from 2.0×10^{-3} mol·dm^{-3} to 5.0×10^{-3} mol·dm^{-3}) were added into the 3 mL solution of the complex (**3a–3c**: from 1.2×10^{-4} mol·dm^{-3} to 2.5×10^{-4} mol·dm^{-3}; **3d**: 5×10^{-4} mol·dm^{-3}) by a syringe, and the spectral changes were recorded by a PGENERAL TU1901 UV−vis spectrophotometer at 298 K. The UV−vis titration experiments in DMSO were the same as those in CH_3CN, expect the concentration of **3a–3d** was changed to 3×10^{-4} mol·dm^{-3}. For a typical ^{1}H NMR titration experiment of **3d** in DMSO-d_6, 0.5 μL aliquots of a tetra-*n*-butylammonium salt ([F^-] = 0.25 mol·dm^{-3}, [OAc^-] = 0.3 mol·dm^{-3} in DMSO-d_6) were added into the 0.5 mL solution of the complex 3d in DMSO-d_6 (9.7×10^{-4} mol·dm^{-3}) by a syringe gradually, and the ^{1}H NMR and ^{19}F NMR spectral changes were recorded by a Varian Mercury-Plus 300 spectrometer at 298 K. The binding constant log K values were determined by nonlinear fitting using 1:1 model.[33] Job's plots were obtained from a series of solutions in which the fraction of the corresponding anions varied, keeping the total concentration (the complexes and anions) constant. The maxima of the plots indicated the binding stoichiometry of the complexes with anions.

Acknowledgements

We acknowledge financial support from the National Natural Science Foundation of China (20971131 and J1103305), the Natural Science Foundation of Guangdong Province (S2012010010566), and Sun Yat-Sen University.

Notes and references

MOE Key Laboratory of Bioinorganic and Synthetic Chemistry, School of Chemistry and Chemical Engineering, Sun Yat-Sen University, Guangzhou 510275, China

E-mail: zhaoxy@mail.sysu.edu.cn., Fax: (+86)020-84112245; Tel: (+86)020-84110062.

† Electronic Supplementary Information (ESI) available: Additional Figures and Tables. CCDC 1028565 (**3a**), 1028514 (**3a·DMF·THF**), 1028592 (**3b·CH_3CN**), and 1028516 (**3c·CH_3CN**). For ESI and crystallographic data in CIF and other electronic format see DOI: 10.1039/xxxxx.

1 (a) P. A. Gale, N. Busschaert, C. J. E. Haynes, L. E. Karagiannidis and I. L. Kirby, *Chem. Soc. Rev*. 2014, **43**, 205–241; (b) F. Wang, L. Wang, X. Chen and Yoon, J. *Chem. Soc. Rev*. 2014, **43**, 4312–4324; (c) L. Fabbrizzi and A. Poggi, *Chem. Soc. Rev*. 2013, **42**, 1681–1699; (d) P. A. Gale, Acc. *Chem. Res.* 2011, **44**, 216−226; (e) Z. Xu, X. Chen, H. N. Kim and J. Yoon, *Chem. Soc. Rev*. 2010, **39**, 127–137; (f) S. Kubik, *Chem. Soc. Rev.* 2010, **39**, 3648–3663; (g) C. Caltagirone and P. A. Gale, *Chem. Soc. Rev.* 2009, **38**, 520; (h) A. P. Davis, *Coord. Chem. Rev.* 2006, **250**, 2939–2951.

2 C. H. Park and H. E. Simmons, *J. Am. Chem. Soc.* 1968, **90**, 2431–2431.

3 (a) N. H. Evans and P. D. Beer *Angew. Chem. Int. Ed*. 2014, **53**, 11716–11754; (b) Z. Guo, I. Shin and J. Yoon, *Chem. Commun.* 2012, **48**, 5956–5967; (c) H. T. Ngo, X. Liu and K. A. Jolliffe, *Chem. Soc. Rev.* 2012, **41**, 4928–4925; (d) R. M. Duke, E. B. Veale, F. M. Pfeffer, P. E. Kruger and T. Gunnlaugsson, *Chem. Soc. Rev.* 2010, **39**, 3936–3953; (e) Steed, J. W. *Chem. Soc. Rev*. 2009, **38**, 506–519.

4 (a) V. Amendola, G. Bergamaschi, M. Boiocchi, L. Fabbrizzi and L. Mosca, *J. Am. Chem. Soc.* 2013, **135**, 6345−6355; (b) L. Fabbrizzi, V. Amendola and L. Mosca, *Chem. Soc. Rev*. 2010, **39**, 3889–3915.

5 A. F. Li, J. H. Wang, F. Wang and Y. B. Jiang, *Chem. Soc. Rev.* 2010, **39**, 3729–3745.

6 (a) M. A. Hossain, R. A. Begum, V. W. Day and K. Bowman-James, *Amide and urea-based receptors. Supramolecular Chemistry: From Molecules to Nanomaterials* Wiley: Hoboken, NJ, 2012, *3*, 1153−1178; (b) C. R. Bondy and S. J. Loeb, *Coord. Chem. Rev.* 2003, **240**, 77–99.

7 M. D. Best, S. L. Tobey and E. V. Anslyn, *Coord. Chem. Rev*. 2003, **240**, 3–15.

8 (a) P. A. Gale and C. Caltagirone, *Chem. Soc. Rev.* 2015, DOI:10.1039 /c4cs00179f. (b) E. B. Veale and T. Gunnlaugsson, *Annu. Rep. Prog. Chem. Sect. B*. 2010, **106**, 376–406.

9 (a) N. H. Evans, C. J. Serpell, K. E. Christensen and P. D. Beer, *Eur. J. Inorg. Chem.* 2012, 939–944; (b) D. P. Cormode, A. J. Evans, J. J. Davis and P. D. Beer, *Dalton.Trans.* 2010, **39**, 6532–6541; (c) Y. Willener, K. M. Joly, C. J. Moody and J. H. R. Tucker, *J. Org. Chem.* 2008, **73**, 1225–1233; (d) F. Oton, A. Tarraga, A. Espinosa, M. D. Velasco and P. Molina, *J. Org. Chem.*, 2006, **71**, 4590–4598; (e) F. Oton, A. Tarraga, M. D. Velasco and P. Molina, *Dalton. Trans.* 2006, 3685–3692; (f) F. Oton, A. Tarraga, M. D. Velasco and P. Molina, *Dalton Trans.* 2005, **7**, 1159–1161; (g) P. D. Beer and S. R. Bayly, *Top. Curr. Chem.* 2005, **255**, 125–162; (h) F. Oton, A. Tarraga, M. D. Velasco, A. Espinosa and P. Molina, *Chem. Commun.* 2004, 1658–1659; (i) H. Miyaji, S. R. Collinson, I. Prokes and J. H. R. Tucker, *Chem. Commun.* 2003, 64–65; (j) A. J. Evans, S. E. Matthews, A. R. Cowley and P. D. Beer, *Dalton Trans.* 2003, **24**, 4644–4650. (k) B. Alonso, C. M. Casado, I. Cuadrado, M. Moran and A. E. Kaifer, *Chem. Commun*, 2002, 1778–1779; (l) P. D. Beer, J. Cadam, J. M. Loris, R. Martinez-Manez, M. E. Padilla, T. Pardo, D. K. Smith and J. Soto, *Dalton Trans.* 1999,127–134.

10 (a) A. Ramdass, V. Sathish, M. Velayudham, P. Thanasekaran, K. L. Lu and S. Rajagopal, *Inorg. Chem. Commun.* 2013, **35**, 186–191; (b) M. O. Odago, A. E. Hoffman, R. L. Carpenter, D. C. T. Tse, S. S. Sun and A. J. Lees, *Inorg. Chim. Acta* 2011, **374**, 558–565.

11 (a) G. Baggi, M. Boiocchi, C. Ciarrocchi and L. Fabbrizzi,*Inorg. Chem.* 2013, **52**, 5273–5283; (b) Y. J. P. Hao, J. Yang, S. G. Li, X. J. Huang, X. J. Yang and B. Wu, *Dalton Trans.* 2012, **41**, 7689–7694; (c) A. Ghosh, S. Verma, B. Ganguly, H. N. Ghosh and A. Das, *Eur. J. Inorg. Chem.* 2009, **2009**, 2496–2507; (d) A. Ghosh, B. Ganguly and A. Das, *Inorg. Chem.* 2007, **46**, 9912–9918.

12 Y. Li, Y. Liu, D. Nam, S. Park, J. Yoon and M. H. Hyun, *Dyes and Pigments*, 2014, **100**, 241–246.

13 (a) C. L. Li, Q. R. Guan, X. C. Li, J. Wang, Y. P. Zhou, D. G. Churchill and H. Y. Chao, *Inorg. Chem. Commun.* 2013, **35**, 149–151; (b) Y. P. Zhou, M. Zhang, Y. H. Li, Q. R. Guan, F. Wang, Z. J. Lin, C. K. Lam, X. L. Feng and H. Y. Chao, *Inorg. Chem.* 2012, **51**, 5099–5109; (c) X. He, F. Herranz, E. C. C. Cheng, R. Vilar and V.

W. W. Yam, *Chem. Eur. J.* 2010, **16**, 9123–9131; (d) X. He and V. W. W. Yam, *Inorg. Chem.* 2010, **49**, 2273–2279.

14 (a) C. M. G. dos Santos and T. Gunnlaugsson, *Dalton. Trans.* 2009, **24**, 4712–4721; (b) C. M. G. dos Santos, P. B. Fernandez, S. E. Plush, J. P. Leonard and T. Gunnlaugsson, *Chem. Commun.* 2007, **32**, 3389–3391.

15 X. He, N. Zhu and V. W. W. Yam, *Dalton. Trans.* 2011, **40**, 9703–9710.

16 (a) C. L. Ho and W. Y. Wong, Coord. Chem. Rev. 2013, **257**, 1614–1649; (b) W. Y. Wong and P. D. Harvey, *Macromol. Rapid Commun.* 2010, **31**, 671–713; (c) W. Y. Wong, *Dalton Trans.* 2007, 4495–4510; (d) W. Y. Wong and C. L. Ho, *Coord. Chem. Rev.* 2006, **250**, 2627–2690.

17 (a) J. Ni, Y. G. Wang, J. Y. Wang, Y. Q. Zhao, Y. Z. Pan, H. H. Wang, X. Zhang, J. J. Zhang and Z. N. Chen, *Dalton. Trans.* 2013, **42**, 13092–13100; (b) X. Zhang, B. Li, Z. H. Chen and Z. N. Chen, *J. Mater. Chem.* 2012, **22**, 11427–11441; (c) J. Ni, X. Zhang, N. Qiu, Y. H. Wu, L. Y. Zhang, J. Zhang and Z. N. Chen, *Inorg. Chem.* 2011, **50**, 9090–9096; (d) Z. M. Hudson, C. Sun, K. J. Harris, B. E. G. Lucier, R. W. Schurko and S. Wang, *Inorg. Chem.* 2011, **50**, 3447–3457; (e) J. Ni, Y. H. Wu, X. Zhang, B. Li, L. Y. Zhang and Z. N. Chen, *Inorg. Chem.* 2009, **48**, 10202–10210; (f) J. Ni, L. Y. Zhang, H. M. Wen and Z. N. Chen, *Chem. Commun.* 2009, **25**, 3801–3803; (g) M. L. Muro, C. A. Daws and F. N. Castellano, *Chem. Commun.* 2008, **46**, 6134–6136; (h) S. C. F. Kui, S. S. Y. Chui, C. M. Che and N. Zhu, *J. Am. Chem. Soc.* 2006, **128**, 8297–8309; (i) W. Lu, M. C. W. Chan, N. Zhu, C. M. Che, Z. He and K. Y. Wong, *Chem. Eur. J.* 2003, **9**, 6155–6166; (j) V. W. W. Yam, K. M. C. Wong and N. Zhu, *J. Am. Chem. Soc.* 2002, **124**, 6506–6507.

18 (a) C. Y. S. Chung and V. W. W. Yam, *Chem. Eur. J.* 2013, **19**, 13182 – 13192; (b) X. Han, L. Z. Wu, G. Si, J. Pan, Q. Z. Yang, L. P. Zhang and C. H. Tung, *Chem. Eur. J.* 2007, **13**, 1231–1239; (c) K. M. C. Wong, W. S. Tang, X. X. Lu, N. Y. Zhu and V. W. W. Yam, *Inorg. Chem.* 2005, **44**, 1492–1498.

19 (a) V. Uahengo, N. Zhou, B. Xiong, P. Cai, K. Hu and G. Cheng, *J. Organmet. Chem.* 2013, **732**, 102–108; (b) K. M. C. Wong and V. W. W. Yam, *Coord. Chem. Rev.* 2007, **251**, 2477–2488; (c) H. S. Lo, S. K. Yip, K. M. C. Wong, N. Zhu and V. W. W. Yam, *Organometallics* 2006, **25**, 3537–3540; (d) K. M. C. Wong, W. S. Tang, X. X. Lu, N. Zhu and V. W. W. Yam, *Inorg. Chem.* 2005, **44**, 1492–1498; (e) W. S. Tang, X. X. Lu, K. M. C. Wong and V. W. W. Yam, *J. Mater. Chem.* 2005, **15**, 2714–2720; (f) P. K. M. Siu, S. W. Lai, W. Lu, N. Zhu and C. M. Che, *Eur. J. Inorg. Chem.* 2003, **15**, 2749–2752; (g) V. W. W. Yam, R. P. L. Tang, K. M. C. Wong, C. C. Ko and K. K. Cheung, *Inorg. Chem.* 2001, **40**, 571–574; (h) V. W. W. Yam, R. P. L. Tang, K. M. C. Wong and K. K. Cheung, *Organometallics* 2001, **20**, 4476–4482; (i) A. Diez, E. Lalinde and M. T. Moreno, *Coord. Chem. Rev.* 2011, **255**, 2426–2447.

20 (a) J. Ni, Y. G. Wang, H. H. Wang, L. Xu, Y. Q. Zhao, Y. Z. Pan and J. J. Zhang, *Dalton. Trans.* 2014, **43**, 352–360. (b) J. Ni, Y. G. Wang, H. H. Wang, Y. Z. Pan, L. Xu, Y. Q. Zhao, X. Y. Liu and J. J. Zhang, *Eur. J. Inorg. Chem*. 2014, 986–993.

21 (a) A. Han, P. W. Du, Z. J. Sun, H. T. Wu, H. X. Jia, R. Zhang, Z. N. Liang, R. Cao and R. Eisenberg, *Inorg. Chem.* 2014, **53**, 3338–3344; (b) X. Zhang, J. Y. Wang, J. Ni, L. Y. Zhang and Z. N. Chen, *Inorg. Chem.* 2012, **51**, 5569–5579;. (c) J. Ni, X. Zhang, Y. H. Wu, L. Y. Zhang and Z. N. Chen, *Chem. Eur. J.* 2011, **17**, 1171–1183

22 (a) Y. J. Tian, E. T. Shi, Y. K. Tian, R. S. Yao and F. Wang, *Org. Lett.* 2014, **16**, 3180–3183; (b) Y. Tanaka, K. M. C. Wong and V. W. W. Yam, *Chem. Eur. J.* 2013, **19**, 390 – 399; (c) Y. Tanaka, K. M. C. Wong and V. W. W. Yam, *Angew. Chem. Int. Ed.* 2013, **52**, 14117–14120; (d) T. Nabeshima, Y. Hasegawa, R. Trokowski and M. Yamamura, *Tetrahedron Lett.* 2012, **53**, 6182–6185; (e) H. Sun, H. Guo, W. Wu, X. Liu and J. Zhao, *Dalton Trans.* 2011, **40**, 7834–7841.

23 (a) L. Liu, S. Guo, J. Ma, K. Xu, J. Zhao and T. Zhang, *Chem. Eur. J.* 2014, **20,** 14282–14295; (b) J. J. Zhong, Q. Y. Meng, G. X. Wang, Q. Liu, B. Chen, K. Feng, C. H. Tung and L. Z. Wu, *Chem. Eur. J.* 2013, **19**, 6443–6450; (c) X. H. Wang, S. Goeb, Z. Q. Ji, N. A. Pogulaichenko and F. N. Castellano, *Inorg. Chem.* 2011, **50**, 705-707; (d) P. Jarosz, P. Du, J. Schneider, S. H. Lee, D. McCamant and R. Eisenberg, *Inorg. Chem.* 2009, **48**, 9653–9663; (e) P. Du, K. Knowles and R. Eisenberg, *J. Am. Chem. Soc.* 2008, **130**, 12576-12577; (f) P. Du, J. Schneider, P. Jarosz and R. Eisenberg, *J. Am. Chem. Soc.* 2006, **128**, 7726-7727; (g) Y. Yang, D. Zhang, L. Z. Wu, B. Chen, L. P. Zhang and C. H. Tung, *J. Org. Chem.* 2004, **69**, 4788-4791; (h) D. Zhang, L. Z. Wu, Q. Z. Yang, X. H. Li, L. P. Zhang, C. H. Tung, *Org. Lett.* 2003, *5*, 3221–3224.

24 (a) E. C. H. Kwok, M. Y. Chan, K. M. C. Wong and V. W. W. Yam, *Chem. Eur. J.* 2014, **20**, 3142–3153; (b) X. Yi, C. Zhang, S. Guo, J. Ma and J. Zhao, *Dalton Trans.* 2014, 43, 1672–1683; (c) W. Wu, L. Liu, X. Cui, C. Zhang and J. Zhao, *Dalton Trans.* 2013, **42**, 14374–14379; (d) Q. Liu, H. Zhan, C. L. Ho, F. R. Dai, Y. Y. Fu, Z. Xie, L. Wang, J. H. Li, F. Yan and S. P. Huang, *Chem. Asian J.* 2013, **8**, 1892–1900; (e) F. R. Dai, H. M. Zhan, Q. Liu, Y. Y. Fu, J. H. Li, Q. W. Wang, Z. Xie, L. Wang, F. Yan and W. Y. Wong, *Chem. Eur. J.* 2012, **18**, 1502–1511; (f) W. Wu, J. Zhao, H. Guo, J. Sun, S. Ji, and Z. Wang, *Chem. Eur. J.* 2012, **18**, 1961–1968; (g) H. M. Zhan, S. Lamare, A. Ng, T. Kenny, H. Guernon, W. K. Chan, A. B. Djurisic, P. D. Harvey and W. Y. Wong, *Macromolecules* 2011, **44**, 5155–5167; (h) W. Y. Wong and C. L.Ho, *Acc. Chem. Res.* 2010, **43**, 1246–1256; (i) E. C. H. Kwok, M. Y. Chan, K. M. C. Wong, W. H. Lam and V. W. W. Yam, *Chem. Eur. J.* 2010, **16**, 12244–12254; (j) W. Y.Wong, *Macromol. Chem. Phys.* 2008, **209**, 14–24; (k) W. Y. Wong X. Z. Wang, Z. He, A. B. Djurisic, C. T. Yip, K. Y. Cheung, H. Wang, C. S. K. Mak, and W. K. Chan, *Nature Mater.* 2007, **6**, 521–527; (l) W. Y. Wong, X. Z. Wang, Z. He, K. K. Chan, A. B. Djurisic, K. Y. Cheung, C. T. Yip, A. M. C. Ng, Y. Y. Xi and C. S. K. Mak, *J. Am. Chem. Soc.* 2007, **129**, 14372–14380; (m) X. Z. Wang, W. Y. Wong, K.Y. Cheung, M. K. Fung, A. B. Djurisic and W. K. Chan, *Dalton Trans.* 2008, 5484–5494; (n) S. Chakraborty, T. J. Wadas, H. Hester, C. Flaschenreim, R. Schmehl and R. Eisenberg, *Inorg. Chem.* 2005, **44**, 6284–6293.

25 (a) Y. Li, D. P. K. Tsang, C. K. M. Chan, K. M. C. Wong, M. Y. Chan and V. W. W. Yam, *Chem. Eur. J.* 2014, **20**, 13710–13715; (b) K. M. C. Wong, M. M. Y. Chan and V. W. W. Yam, *Adv. Mater.* 2014, **26**, 5558–5568; (c) E. S. H. Lam, A. Y. Y. Tam, M. Y. Chan and V. W. W. Yam, *Isr. J. Chem.* 2014, **54**, 986–992. (d) E. S. H. Lam, D. P. K. Tsang, W. H. Lam, A. Y. Y. Tam, M. Y. Chan, W. T. Wong and V. W. W. Yam, *Chem. Eur. J.* 2013, **19**, 6385–6397; (e) L. Ho, C. H. Chui, W. Y. Wong, S. M. Aly, D. Fortin, P. D. Harvey, B. Yao, Z. Xie and L. Wang, *Macromol. Chem. Phys.* 2009, **210**, 1786–1798; (f) W. Y. Wong, G. J. Zhou, Z. He, K. Y. Cheung, A. M. C. Ng, A. B. Djurisic andW. K. Chan, *Macromol. Chem. Phys.* 2008, **209**, 1319–1332; (g) S. C. Chan, M. C. W. Chan, Y. Wang, C. M. Che, K. K. Cheung and N. Y. Zhu, *Chem. Eur. J.* 2001, **7**, 4180–4190.

26 (a) G. J. Zhou and W. Y. Wong, *Chem. Soc. Rev.* 2011, **40**, 2541–2566; (b) G. J. Zhou, W. Y. Wong, S.Y. Poon, C. Ye and Z. Lin, *Adv. Funct. Mater.* 2009, **19**, 531–544; (c) T. M. Pritchett, W. F. Sun, F. Q. Guo, B. G. Zhang, M. J. Ferry, J. E. Rogers-Haley, W. III. Shensky and A. G. Mott, *Opt. Lett.* 2008, **33**, 1053–1055; (d) Z. Q. Ji, Y. J. Li and W. F. Sun, *Inorg. Chem.* 2008, **47**, 7599–7607; (e) G.

J. Zhou, W. Y. Wong, C. Ye and Z. Lin, *Adv. Funct. Mater.* 2007, **17**, 963–975; (f) G. J. Zhou, W. Y. Wong, Z. Lin and C. Ye, *Angew. Chem. Int. Ed.* 2006, **45**, 6189–6193; (g) G. J. Zhou, W. Y. Wong, D. Cui and C. Ye, *Chem. Mater.* 2005, **17**, 5209–5217; (h) F. Q. Guo, W. F. Sun, Y. Liu and K. Schanze, *Inorg. Chem,* 2005, **44**, 4055–4065; (i) W. F. Sun, Z. X. Wu, Q. Z. Yang, L. Z. Wu and C. H. Tung, *Appl. Phys. Lett.* 2003, **82**, 850–852.

27 (a) M. C. L. Yeung, B. W. K. Chu and V. V. W. Yam, *ChemistryOpen* 2014, **3**, 172–176. (b) C. Y. S. Chung and V. W. W. Yam, *Chem. Eur. J.* 2014, **20**, 13016–13027; (c) X. X. Lin, Z. H. Li, X. Y. Huang, Y. Jiang, Q. H. Wei and G. N. Chen, *Dalton Trans.* 2014, **43**, 8861-8867; (d) J. L. Fillaut, H. Akdas-Kilig, E. Dean, C. Latouche and A. Boucekkine, *Inorg. Chem.* 2013, **52**, 4890–4897; (e) C. Qin, W. Y. Wong and L. Wang, *Macromolecules* 2011, **44**, 483; (f) S. Shanmugaraju, A. K. Bar, K. W. Chi and P. S. Mukherjee, *Organometallics* 2010, **29**, 2971–2980; (g) Y. Fan, Y. M. Zhu, F. R. Dai, L. Y. Zhang and Z. N. Chen, *Dalton Trans.* 2007, **35**, 3885–3892.

28 (a) Y. Cao, M. O. Wolf and B. O. Patrick, *Inorg. Chem.* 2013, **52**, 5636–5638; (b) G. S. M. Tong, Y. C. Law, S. C. F. Kui, N. Zhu, K. H. Leung, D. L. Phillips and C. M. Che, *Chem. Eur. J.* 2010, **16**, 6540–6554; (c) J. Ni, L. Y. Zhang, and Z. N. Chen, *J. Organomet. Chem.* 2009, **694**, 339–345; (d) E. Shikhova, E. O. Danilov, S. Kinayyigit, I. E. Pomestchenko, A. D. Tregubov, F. Camerel, P. Retailleau, R. Ziessel and F. N. Castellano, *Inorg. Chem.* 2007, **46**, 3038-3048; (e) H. S. Lo, S. K. Yip, K. M. C. Wong, N. Zhu and V. W. W. Yam, *Organometallics* 2006, **25**, 3537–3540; (f) K. M. C. Wong, W. S. Tang, B. W. K. Chu, N. Zhu and V. W. W. Yam, *Organometallics*, 2004, **23**, 3459 –3465; (g) V. W. W. Yam, K. M. C. Wong, N. Zhu, *J. Am. Chem. Soc.* 2002, **124**, 6506–6507.

29 S. Y. L. Leung, A. Y. Y. Tam, C. H. Tao, H. S. Chow, and V. W. W. Yam, *J. Am. Chem. Soc.* 2012, **134**, 1047−1056.

30 (a) D. E. Gomez, L. Fabbrizzi, M. Licchelli and E. Monzani, *Org. Biomol. Chem.* 2005, **3**, 1495 − 1500; (b) D. Esteban-Gomez, L. Fabbrizzi and M. Liechelli, *J. Org. Chem.* 2005, **70**, 5717−5720; (c) M. Boiocchi, L. Del Boca, D. Esteban-Gomez, L. Fabbrizzi, M. Licchelli and E. Monzani, *Chem. Eur. J.* 2005, **11**, 3097−3104; (d) M. Boiocchi, L. Del Boca, D. E. Gomez, L. Fabbrizzi, M. Licchelli and E. Monzani, *J. Am. Chem. Soc.* 2004, **126**, 16507−16514.

31 S. W. Lai, M. C. W. Chan, K. K. Cheung and C. M. Che, *Inorg. Chem.* 1999, **38**, 4262–4267.

32 O.V. Dolomanov, L. J. Bourhis, R. J. Gildea, J.A. K. Howard and H. Puschmann, OLEX2: A complete structure solution, refinement and analysis program.*J. Appl. Cryst.*, 2009, **42**, 339–341.

33 J. Bourson, J. Pouget and B. Valeur, *J. Phys. Chem.* 1993, **97**, 4552−4557.

Graphical Abstract

The relationship between the structure and anion-binding ability of platinum(II) acetylide complexes with urea group has been studied.